Determination of Clear-Sky Radiative Flux Profiles, Heating Rates, and Optical Depths Using Unmanned Aerospace Vehicles as a Platform

FRANCISCO P. J. VALERO AND SHELLY K. POPE

Atmospheric Research Laboratory, Scripps Institution of Oceanography, University of California, San Diego, La Jolla, California

ROBERT G. ELLINGSON

University of Maryland, Department of Meteorology, College Park, Maryland

ANTHONY W. STRAWA

NASA/Ames Research Center, Moffett Field, California

JOHN VITKO JR.

Sandia National Laboratories, Livermore, California

(Manuscript received 3 October 1995, in final form 22 March 1996)

ABSTRACT

In this paper the authors report results obtained using an unmanned aerospace vehicle (UAV) as an experimental platform for atmospheric radiative transfer research. These are the first ever climate measurements made from a UAV and represent a major step forward in realizing the unique potential of long-endurance, high-altitude UAVs to contribute to climate and environmental studies. Furthermore, the radiative flux divergences determined during these experiments are some of the highest quality measurements of this kind obtained from any type of aircraft and constitute an important test of radiative transfer models.

1. Introduction

The interaction of the earth's solar and thermal radiation with clouds is the dominant uncertainty in atmospheric climate models and accounts for most of the factor of 3 uncertainty in predicted temperature rise for a doubling of CO_2 (Cess et al. 1989). Reduction of these uncertainties will require an improved understanding of radiation–cloud interactions. Ground- and space-based programs to characterize these interactions are now underway. However, certain key parameters such as the radiative flux profiles and atmospheric heating rates must be measured in situ and, hence, require airborne measurements. Furthermore, to be of maximum use, these measurements must be made up to the tropical tropopause (an altitude of 20 km) and for periods of 24 h or more to characterize diurnal effects accurately. Recently emerged long-endurance, high-altitude unmanned aerospace vehicles (UAVs) appear to have unique potential for making such measurements.

Therefore, we have embarked on a program to demonstrate and use UAVs for atmospheric research. Our primary objectives include 1) the direct measurement of radiative flux profiles with sufficient accuracy to use not only as reliable experimental information but also as reference in the testing and validation of radiative transfer models, 2) the calibration of satellites, and 3) the validation of satellite-derived radiative parameters. Accurate measurement of radiative flux profiles leads naturally to the determination of atmospheric radiative flux divergence and heating rate profiles, quantities that are recognized as fundamental to the understanding of atmospheric processes, cloud physics, and climate.

It should be noted that for determination of flux divergence and atmospheric heating rates, the intercomparability of the instruments is critical. In these experiments the intercomparability was excellent, as one set of identically calibrated radiometers was stepped through altitude to yield measurement profiles.

In the following sections we present measurements of infrared and solar radiative flux profiles, heating rates, and multispectral optical depths as well as comparisons with infrared and solar model calculations.

The series of experiments that we discuss here were made at two different sites, the Edwards Air Force Base

Corresponding author address: Shelly K. Pope, Scripps Institution of Oceanography, University of California, San Diego, 9500 Gilman Dr., Dept. 0242, La Jolla, CA 92093-0242.

FIG. 1. Photo of the UAV with radiometers installed. One solar broadband, one infrared broadband, and one TDDR are in the top, looking upward. Another solar-infrared broadband pair is installed in the bottom, looking downward. The landing gear is retracted for cruise and ascents and extended for descents and landing.

in southern California (13 November 1993) and the Department of Energy (DOE) Clouds and Radiation Testbed (CART) site in Oklahoma (April 1994). The experiments were part of the DOE's Atmospheric Radiation Measurement (ARM) Program. Originally planned as a demonstration of the capability of UAVs to support future sophisticated and complex observation programs, these experiments provided us the opportunity to make focused radiation measurements of the highest quality as the result of the combination of UAVs and state-of-the-art experimental methods, instruments, and model calculations.

2. Instrumentation

The radiation instruments included up- and downlooking, broad spectral bandpass (4–30 μm) hemispherical field-of-view, infrared radiometers, an improved version of those described by Valero et al. (1982); up- and downlooking solar, broad spectral bandpass (0.3–2.8 μm) hemispherical field-of-view radiometers; and an uplooking, seven-spectral-channel (380, 412, 500, 675, 862, 1064, and 1640 nm), total-direct-diffuse radiometer, or TDDR (Valero et al. 1989; Valero and Pilewskie 1992). This instrument complement provides broadband infrared and solar fluxes, and direct, diffuse, and total fluxes in seven spectral channels in the solar wavelength range.

The radiation instrumentation was integrated in the General Atomics UAV. The payload construction and integration, including electronics, power, and telemetry systems, was carried out by Sandia National Laboratories. Data acquired in flight were telemetered to the ground in real time and displayed in the ground station. Housekeeping information as well as the raw data from all instruments were monitored to evaluate the system performance as the data were being acquired. A photograph of the UAV with the radiation instrumentation mounted is shown in Fig. 1.

To complete the measurement set, an infrared (4–30 μm) hemispherical field-of-view radiometer was located at the CART site to measure downwelling infrared flux. This instrument was similar to the airborne radiometers except that a thermoelectric cooler was employed to keep the instrument at a temperature of +10°C and the measurement was constantly referenced to a blackbody at liquid nitrogen temperature, providing a well known and stable reference flux.

Radiometric calibrations were made in our laboratory and in the field before and after the field experiments. To calibrate the infrared instruments, the radiometers were placed in the mouth of a blackbody cone

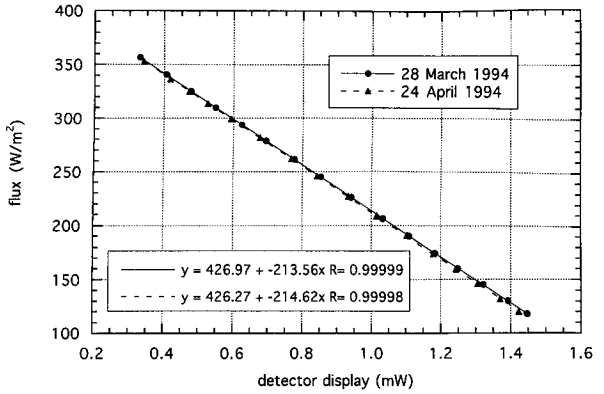

FIG. 2. Calibration results for one of the infrared broadband radiometers, before and after the April flights. The abscissa is the signal from the detector and the ordinate is the corresponding blackbody flux over the spectral interval 4–30 μm. The solid lines are linear fits to the data (symbols).

that sits in a thermal bath. Over several hours the temperature of the bath was varied smoothly from approximately 225 to 290 K in 3–5-K steps, and the radiometer signal as a function of the temperature was recorded. A linear relationship between signal and the blackbody flux results. The calibrations performed before and after the field campaign at the Oklahoma CART site are plotted for one of our infrared radiometers in Fig. 2. Note the superb relative accuracy of the calibrations (less than 1%), which is typical of these instruments. The ground-based infrared radiometer was calibrated on the same calibration apparatus using identical procedures to ensure consistency of measurements.

The solar hemispherical field-of-view radiometers were calibrated by comparison with a cavity radiometer, looking at the sun on a clear day. The diffuse component of the radiation field (incident on the hemispherical FOV radiometers) was measured by using a shadow disk to block the direct solar beam. This diffuse component was subtracted from measurements of the total radiation field to yield a measurement of the direct solar beam. This quantity was then compared with the reading of the cavity radiometer, which measures only the direct beam. (The cavity radiometer was intercompared with reference instruments by its manufacturer and was also intercompared with a reference radiometer from the National Renewable Energy Laboratory.) This comparison, done both before and after the field measurements were taken, yields a multiplicative constant relating radiometer signal to flux. Calibration accuracy is estimated to be about one percent.

The multichannel TDDR is generally calibrated using the Langley plot method. However, for the purposes of these experiments we preferred to use a differential approach to determine the optical depth of atmospheric layers; at a given altitude the optical depth of the total overlying atmosphere was measured, then was subtracted from the optical depth measured similarly (and with the same instrument) at a lower altitude. This approach reduces the determination of the optical depth of atmospheric layers to a relative measurement, independent of exoatmospheric constants, of direct beam intensities above and below the layer of interest. The TDDR is also used to determine direct/diffuse ratios needed to correct solar fluxes for aircraft flight attitude and navigational variations.

3. Experiments

The conceptual flight profile intended to observe radiative fluxes and flux divergence is represented in Fig. 3. For the Oklahoma flights, the aircraft spent about 10 min at each level, tracing out a bow-tie pattern centered over the CART site. The November flight in California was primarily an engineering test flight and so did not conform exactly to this ideal flight plan. The general idea behind such profiles is to have horizontal, wings-level tracks to minimize the corrections in the measured fluxes that are necessitated by changing aircraft attitude due to turns, climbs, and descents. These level legs are also useful as a reference when additional data need to be retrieved from nonlevel portions of the flight. In addition, most of the CART site flights were flown near local noon to minimize the effects of varying solar zenith angle, surface temperature, and underlying albedo.

These first missions were designed primarily for clear sky conditions, where clear sky means less than about 20% visible cloud cover. One reason for this is the need to address questions raised recently concerning the accuracy of clear-sky calculations (e.g., Ellingson et al. 1991). The other primary reason is that in the absence of large horizontal gradients of atmospheric thermodynamic variables clear sky conditions enable the measurement of a valid radiative flux profile

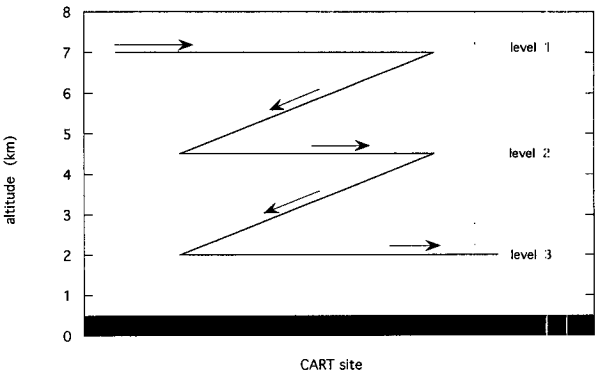

FIG. 3. Diagram of the conceptual flight profile for the UAV. The maximum altitude of this UAV is 7 km (23 000 ft). The minimum altitude is determined by line-of-sight requirements for the tracking antenna.

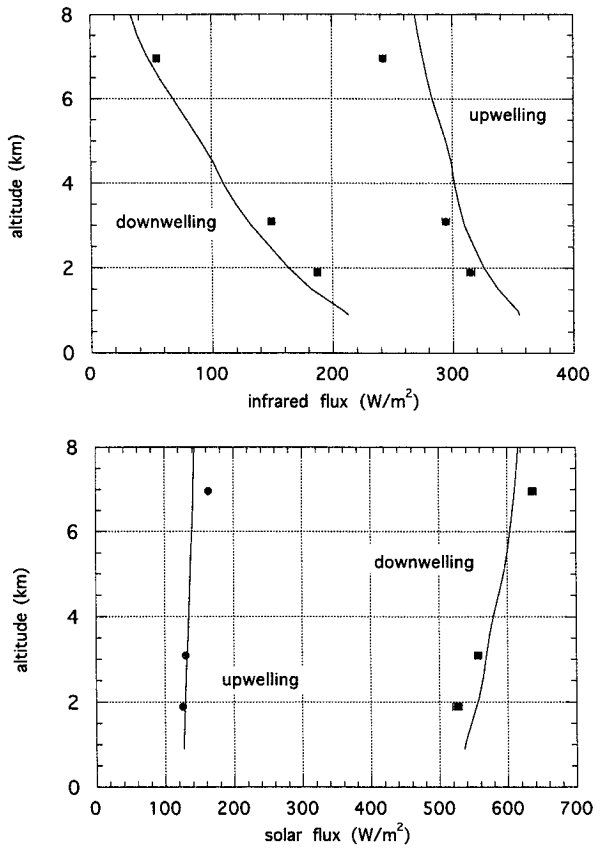

FIG. 4. Fluxes as a function of altitude on 13 November 1993 over Edwards Air Force Base in southern California. The symbols are the measurements and the solid lines represent the model calculation. The downwelling solar profile is normalized to a solar zenith angle of 61°.

with a single UAV simply by stepping the aircraft through altitude over the same geographical location.

Aircraft operations required that under certain conditions the landing gear be extended. During such times corrections for the effect of the landing gear on the upwelling solar and infrared broadband fluxes are made. When extended, the gear reduces the signal by about 21% in the solar and by about 2% in the infrared. Most of the data were collected with the gear retracted and so do not require this correction.

The effects of aircraft turns on the downwelling solar flux can be calculated and appropriate corrections can be made as follows. The zenith angle of the sun with respect to the earth, ϕ_E, is calculated using the procedure outlined by Michalsky (1988). The zenith angle of the sun with respect to the aircraft (i.e., with respect to the detector) ϕ_A is calculated using the aircraft navigational data, including pitch, roll, and heading (Hammer et al. 1991). The ratio of cosine ϕ_E to cosine ϕ_A corrects for aircraft deviations from level flight and is applied only to the direct, not to the diffuse, component of the solar flux. (The direct/diffuse ratio needed for this correction is determined from the TDDR data.) Uncertainties in the aircraft navigational data translate directly into uncertainty in the downwelling solar flux. The error bars in the data plots (Figs. 4–6) indicate the estimated uncertainty due to all the factors discussed above in addition to some smoothing done over altitude.

4. Models

The vertical temperature and water vapor profiles used in the calculations were specified from radiosonde data obtained during the flights. Climatological values were chosen for the remaining trace gas constituents. Solar-weighted surface albedo values of 0.22 for Oklahoma and 0.24 for Edwards were used, having been deduced from the observations. The surface emissivity was taken to be 1.0. No aerosols were included.

The solar calculations were performed with MODTRAN3 (Anderson et al. 1994). The infrared calcu-

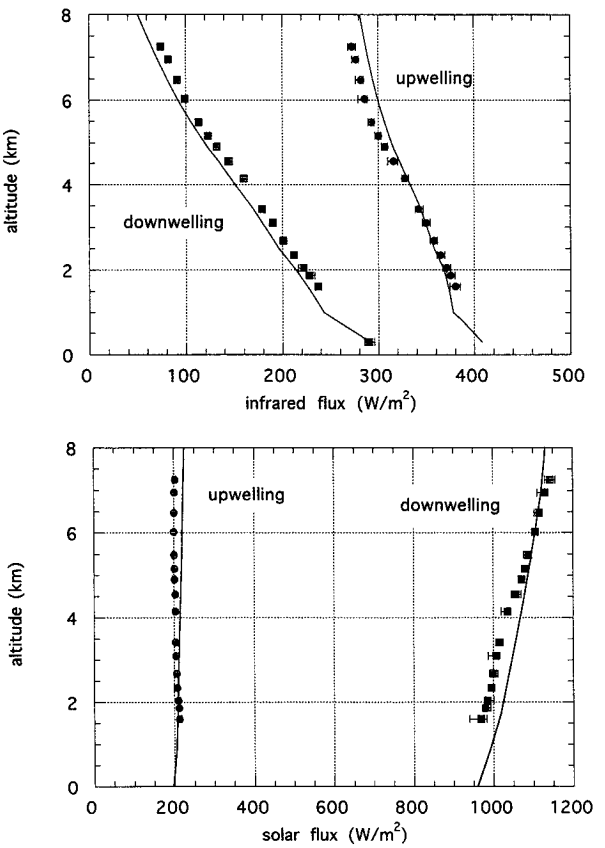

FIG. 5. Fluxes as a function of altitude on 19 April 1994 over the CART site in Oklahoma. The downwelling solar profile is normalized to a solar zenith angle of 26°. The point and error bar at ground level (0.3 km) in the downwelling infrared represents the range of values observed on the ground during that portion of the UAV flight, a period of 1.5 h.

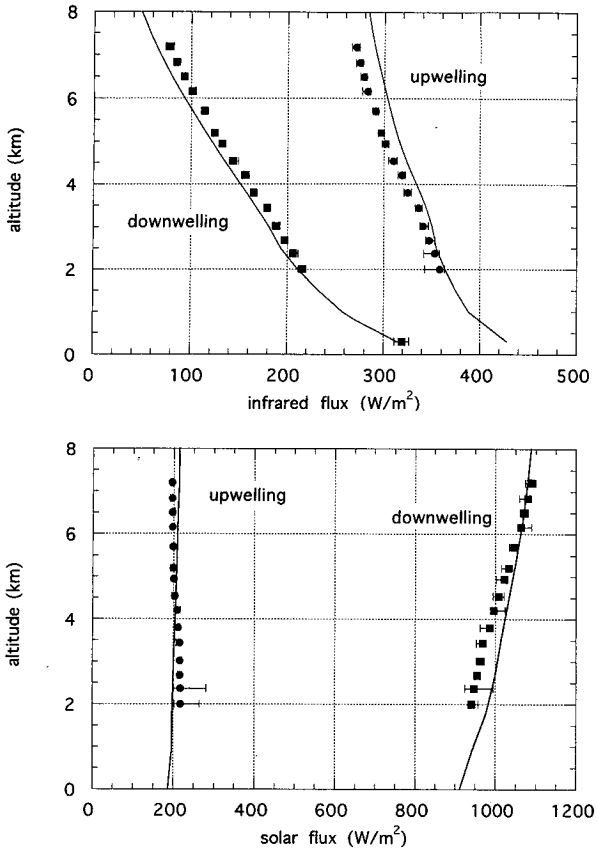

FIG. 6. Fluxes as a function of altitude on 20 April 1994 over the CART site in Oklahoma. The downwelling solar profile is normalized to a solar zenith angle of 30°. The point and error bar at ground level in the downwelling infrared represents the range of values observed on the ground during that portion of the UAV flight, a period of 2 h. Note the larger error bars on the points around 2 km, which result from the clouds moving into the area.

lations were performed with the Clough et al. (1992) line-by-line radiation code LBLRTM, version 3.2, continuum version 2.4, using the HITRAN spectral line database (Rothman et al. 1992). Over the 4–30-μm bandpass, the direct component of the solar flux makes a small but important contribution to the downward infrared flux; the added solar flux was included in results shown herein using calculations from MODTRAN3.

5. Results

Representative examples of the measurements and calculations of radiative flux profiles are shown in Figs. 4–6. The 13 November case (California) is depicted in Fig. 4. This was a "pristine" clear day over the desert. In Fig. 4a we have plotted the experimental results (symbols) and the line-by-line calculation (solid line) for the infrared while Fig. 4b shows the same for the solar. Although there is reasonable overall agreement, the observed fluxes do differ from the model calculations by as much as 30 W m^{-2}. The measurement error bars on most of the data points are smaller than the symbols but it must be kept in mind when considering these points as a profile that as this was an engineering flight the aircraft did not adhere to a well-defined flight track. The points were not taken over the exact same location and are also separated in time by about one hour (from top to bottom). The aircraft was not always in a stable, wings-level attitude, and there are likely positional and navigational uncertainties that are not well enough known to include in an error estimate. At the same time there are uncertainties in the model computations. The temperature profile used in the model was taken from a radiosonde launched from a location some 20 km from the UAV flight path and at a time one hour earlier than the flight. In addition, the ground in this location was covered by a mix of desert vegetation, sand, and rocks, which makes estimates of the surface emissivity and albedo problematic.

The April experiments were performed over the southern Great Plains CART site located in Oklahoma. The 19 April flight occurred on a relatively clear day with some haze and thin cirrus. The comparison between the measured and calculated infrared fluxes is given in Fig. 5a, and Fig. 5b shows the solar fluxes. As this figure and Fig. 6 show, the agreement between model and experimental results has improved for the data taken in Oklahoma. In these instances the aircraft flew on a well-determined track that was essentially collocated (and coincident) with the radiosonde. In addition, the navigational data giving the aircraft position and attitude were of good quality.

The day 20 April was an initially clear-sky day that became more hazy as low-level cumulus clouds moved into the area. The clouds were in a layer from about 4000 to 6000 ft (about 1–2 km.). The 20 April 1994 case is shown in Fig. 6.

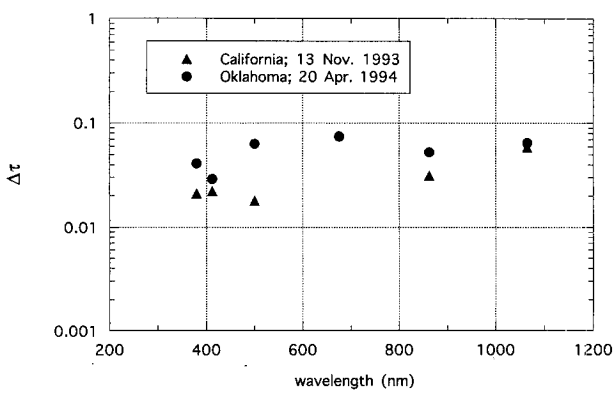

FIG. 7. Optical depth of a layer from 2 to 7 km as a function of wavelength for the two days and locations as labeled.

The spectral dependence of optical depths measured during the 13 November 1993 and 20 April 1994 cases is plotted in Fig. 7. The values plotted are optical depths of a layer from 2 to 7 km. The difference in the optical depths reflects the pristine clear conditions with only some background aerosol present in the 13 November case and the hazy conditions of 20 April in the CART site.

Heating rate profiles deduced from the data discussed above are shown in Figs. 8 and 9. For 20 April separate profiles are calculated for the ascent and the descent portions of the flight. The effects of the changing cloud conditions can be seen at altitudes below about 5 km; small cumulus clouds moved into the observation area during the descent from 7 to 4 km. Thus, not all of the observations are taken over the same conditions. This has a marked effect on the apparent solar heating rate due to the increased effective albedo of the underlying atmosphere as the cloudiness increased.

The results shown here, though only a small sampling of the UAV dataset, clearly establish the capability of the instrumented UAV to make state-of-the-art radiation flux profiling measurements.

The complete dataset covers five days of clear skies with varying humidity and aerosol concentration. Data from the UAV instrumentation as well as from the extensive suite of ground-based instruments located at the CART site have been placed in the ARM archive and are available by contacting Sue Havre of Pacific Northwest Laboratory.

6. Discussion

Our objective was to achieve radiation measurements in the atmosphere of sufficient quality, such that 1) they could be relied upon as accurate and unambiguous, and 2) they could be used to determine atmospheric radiative flux divergence and heating rate pro files. Using the UAV as a platform we have achieved this goal for the clear or almost-clear sky conditions discussed above. The approach taken in these experiments, while effective in the case of clear skies with very slow changes in atmospheric conditions, will most likely not work when inhomogeneous and changing cloud fields are present. This is a consequence of the fact that in the time it takes for the aircraft to change altitudes, the scene observed at one level in the profile is not necessarily the same observed at a different altitude except in very special cases. Also, even in clear skies the change in sun elevation with time results in a continuous change in

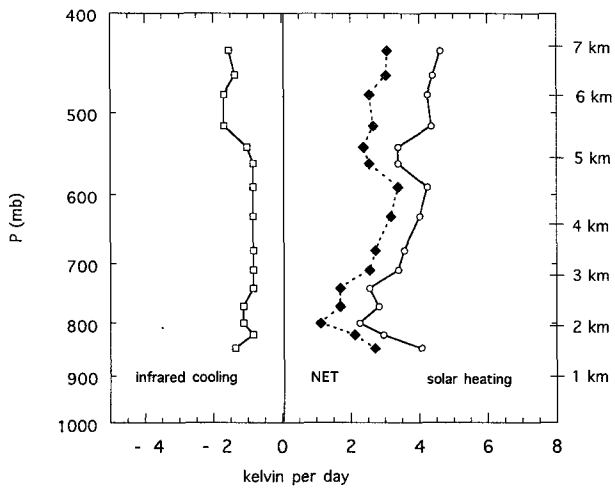

FIG. 8. Instantaneous heating rate profile for 19 April 1994.

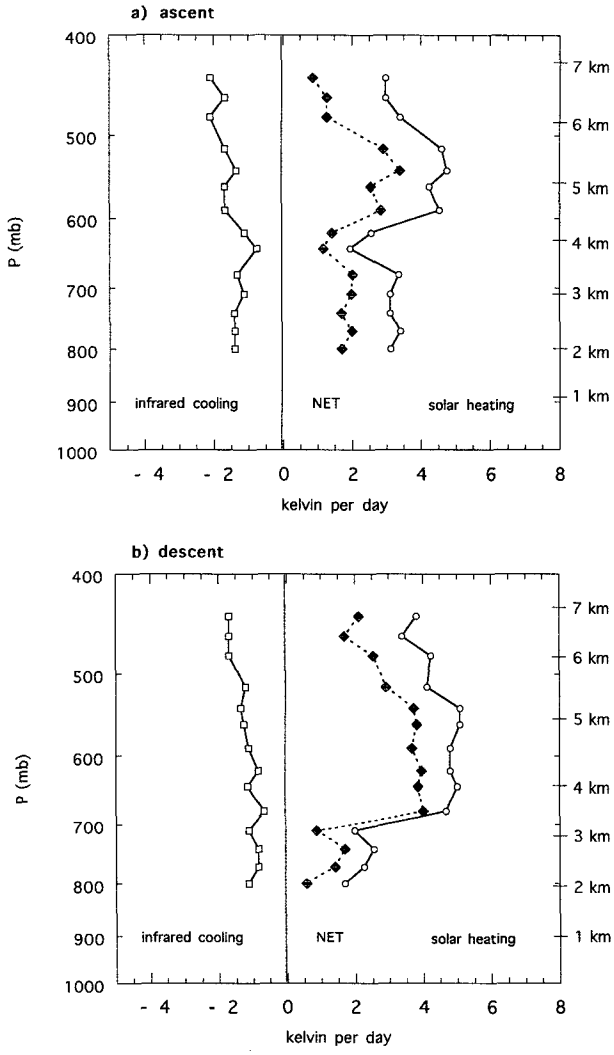

FIG. 9. Instantaneous heating rate profile for (a) the ascent portion of the 20 April 1994 flight, made in relatively clear sky conditions, and (b) the descent portion of the flight, made over a layer of scattered cumulus.

surface temperature, particularly over land, that affects the upwelling infrared flux in a way that is difficult to evaluate accurately without concurrent surface observations. Naturally, solar fluxes are continuously changing with sun elevation.

A way to eliminate most of these uncertainties is to use multiple aircraft that are distributed in altitude to sample the atmospheric column simultaneously at all the altitudes of interest. We have tried the latter approach during the Tropical Oceans Global Atmosphere Coupled Ocean–Atmosphere Response Experiment and Central Equatorial Pacific Experiment projects, us ing conventional aircraft, with excellent results (Pilewskie and Valero 1995). The intent is to use this dual aircraft approach in future UAV flights. With the pilot on the ground instead of in the aircraft, UAVs should be better suited than conventional aircraft for these types of long duration missions and flights over remote areas. With the increased altitude capability under development now, UAVs can be used as a platform for studying radiation–cloud interactions that bridges the gap between manned aircraft and satellites.

Acknowledgments. This work was funded through the Strategic Environmental Research and Development Program and was also supported in part by the Environmental Sciences Division of the U.S. Department of Energy as part of the Atmospheric Radiation Measurement Program.

REFERENCES

Anderson, G. P., and Coauthors, 1994: MODTRAN2: Evolution and applications. *Proc. SPIE Int. Soc. Opt. Eng.,* **2222,** 790–799.

Cess, R. D., and Coauthors, 1989: Interpretation of cloud–climate feedback as produced by 14 atmospheric general circulation models. *Science,* **245,** 513–516.

Clough, S. A., M. J. Iacono, and J.-L. Moncet, 1992: Line-by-line calculation of atmospheric fluxes and cooling rates: Application to water vapor. *J. Geophys. Res.,* **97,** 15 761–15 785.

Ellingson, R. G., J. Ellis, and S. Fels, 1991: The intercomparison of radiation codes in climate models (ICRCCM): Longwave results. *J. Geophys. Res.,* **96,** 8929–8953.

Hammer, P. D., F. P. J. Valero, and S. Kinne, 1991: The 27–28 October 1986 FIRE cirrus case study: Retrieval of cloud particle sizes and optical depths from comparative analyses of aircraft and satellite-based infrared measurements. *Mon. Wea. Rev.,* **119,** 1673–1692.

Michalsky, J. J., 1988: *The Astronomical Almanac*'s algorithm for approximate solar position (1950–2050). *Sol. Energy,* **40,** 227–235.

Pilewskie, P., and F. P. J. Valero, 1995: Direct observations of excess solar absorption by clouds. *Science,* **267,** 1626–1629.

Rothman, L. S., and Coauthors, 1992: HITRAN molecular database: Edition '92. *J. Quant. Spectrosc. Radiat. Transfer,* **48,** 469–508.

Valero, F. P. J., and P. Pilewskie, 1992: Latitudinal survey of spectral optical depths of the Pinatubo volcanic cloud—Derived particle sizes, columnar mass loadings, and effects on planetary albedo. *Geophys. Res. Lett.,* **19,** 163–166.

——, W. J. Y. Gore, and L. P. Giver, 1982: Radiative flux measurements in the troposphere. *Appl. Opt.,* **21,** 831.

——, T. P. Ackerman, and W. J. Y. Gore, 1989: The effects of the arctic haze as determined from airborne radiometric measurements during AGASP II. *J. Atmos. Chem.,* **9,** 225–244.